Preparation and characterization of LaNiO₃ films grown by metal–organic deposition

YAO WANG, GUOFANG ZHANG*, CHENGSHAN LI[†], GUO YAN[†] and YAFENG LU[†]

Key Laboratory of Applied Surface and Colloid Chemistry (Shaanxi Normal University), Ministry of Education, Xi'an 710062, P.R. China; School of Chemistry and Chemical Engineering, Shaanxi Normal University, Xi'an 710062, P.R. China
[†]Northwest Institute for Nonferrous Metal Research, Xi'an 710016, P.R. China

Abstract. **We have investigated the synthesis and characterization of LaNiO₃ (LNO) layers deposited on YSZ (100) substrate by metal–organic deposition (MOD). Texture, morphology and electrical properties of the LaNiO₃ films were characterized by X-ray diffraction (XRD), atomic force microscopy (AFM), scanning electron microscopy (SEM) and electrical resistivity measurement. It has been found that the formation of (h00) orientation depends on pyrolysis temperature, annealing temperature and thickness of LaNiO₃ layers. The LaNiO₃ films prepared under optimal condition indicate highly (h00) orientation and a rather smooth surface. The LaNiO₃ films show a metallic behaviour in the measured temperature range.**

Keywords. **Conductive films; LaNiO₃; metal–organic deposition; texture.**

1. Introduction

In recent decades, high-temperature superconducting coated conductors based on YBa₂Cu₃O₇₋δ (YBCO) have attracted great interest for electric power application (Larbalestier *et al* 2001). The orientation and microstructure of buffer layers between substrate and superconducting layer are very critical to the textured growth and the superconducting performance of YBCO layers. Preparation of buffer layers with high quality, therefore, becomes rather important in order to transfer the texture from substrate into YBCO layer and to realize chemical barriers between the metal substrate and superconducting layer. The considerations for candidates of buffer layers usually include lattice matching, structural and chemical compatibility with the metal substrate and YBCO (Knoth *et al* 2007). A number of electrical insulating buffer layers have been tested so far, but conductive buffer layers have huge commercial prospects because of their potential engineering applications for superconductors. Among many conductive buffer layers, LaNiO₃ (LNO) has been proved to be a good candidate because it exhibits perovskite structure with a lattice parameter (a = 0·384 nm) close to that of YBCO and high conductivity over a wide temperature range (Lee *et al* 1993; Bhuiyan *et al* 2006).

During past years, many kinds of deposition methods, such as pulsed laser deposition (PLD) (Sanchez *et al* 2000; Berini *et al* 2007), sputtering (Wakiya *et al* 2002), mist plasma evaporation (MPE) (Huang *et al* 2004), sol–gel process (Miyake *et al* 2002; Yu *et al* 2004) and chemical solution deposition (CSD) (Li *et al* 1996; Meng *et al* 2000; Zhang *et al* 2000; Bao *et al* 2003; Escote *et al* 2003; Miyazaki *et al* 2004), have been employed for preparation of LaNiO₃ films on several kinds of substrates especially for electrode materials in microelectric devices. Among these deposition routes, chemical solution deposition is simpler and enables easier control over the stoichiometry of the final product than the physical methods. The MOD method has a number of advantages in comparison with other deposition methods and has extensively been used for the preparation of a variety of buffer layers in high-temperature superconducting YBCO-based coated conductors. In order to develop a kind of electrode in ferroelectric substrates, polycrystalline MOD–LaNiO₃ films on Si (111) and quartz substrates were first prepared with the 2-ethyl hexanotes of lanthanum and nickel dissolved in xylene, where the lowest annealing temperature for crystallization is about 530°C (Li *et al* 1996). If the appropriate thermal processing was chosen for the LaNiO₃ films on the SiO₂ glass substrates, the strong (100) orientation of LNO films could be obtained (Miyake *et al* 2002). Meanwhile, epitaxial LaNiO₃ films on single crystalline substrates including SrTiO₃ and LaAlO₃ were successfully prepared by the MOD method (Li *et al* 1996; Cho *et al* 1997). However, the normally used lanthanum precursor La(III) 2-methoxyethoxide is relatively expensive in comparison with simpler La(III) salts such

*Author for correspondence (gfzhang@snnu.edu.cn)

as La(III) nitrate or La(III) acetate, and the solvent 2-methoxyethanol is toxic; they are, therefore, unsuitable for large-scale preparation of NGO buffer layers.

In this study we employed the relatively cheaper $La(NO_3)_3 \cdot 6H_2O$ and $Ni(CH_3COO)_3 \cdot 4H_2O$ as precursors as well as acetic acid as a solvent, and systematically studied the preparation and structure of $LaNiO_3$ films on YSZ (100) substrate, which could serve a buffer layer for coated conductors. We found that pyrolysis temperature, annealing temperature and film thickness are key factors for obtaining the highly (h00) oriented LNO films. The LNO films by MOD show a metallic behaviour measured by transport measurement.

2. Experimental

The $LaNiO_3$ precursor solution was prepared by the method as described in Yu *et al* (2004). Lanthanum nitrate $[La(NO_3)_3 \cdot 6H_2O]$ and nickel acetate $[Ni(CH_3COO)_3 \cdot 4H_2O]$ (99%; both from Alfa Aesar) were used as educts and acetic acid ($\geq 99\%$; Alfa Aesar) as a solvent. For preparing a precursor solution, powders of $La(NO_3)_3 \cdot 6H_2O$ and $Ni(CH_3COO)_3 \cdot 4H_2O$ were mixed in stoichiometric ratio of 1 : 1, and then acetic acid was added. After heating at 70°C for 30 min, a stable green solution was obtained. The concentration of the precursor solution was adjusted to $c = c_{(La^{3+})} = c_{(Ni^{2+})} = 0 \cdot 3$ M. Before preparation of LNO films, the powder derived from LNO gel was investigated to determine the phase formation of $LaNiO_3$. The precursor films were deposited by spin process on YSZ (100) substrates at 3000 rpm for 30 s. The precursor films were heat-treated at a temperature range from 300°C to 450°C for 5 h to pyrolyse organic materials, and then the annealing step was carried out at various temperatures $T = 500$–800°C with 5 K min^{-1} heating rate for 3 h in air to obtain crystallized films in a horizontal furnace. After annealing the samples were cooled in the furnace down to room temperature with 2 K min^{-1} cooling rate. Phase and orientation of films were characterized by 2θ scans of X-ray diffraction with CuKα radiation on a diffractometer. The surface morphology of LNO films was investigated using atomic force microscopy (AFM) and scanning electron microscopy. The temperature dependence of the electrical resistivity of these films was measured by using the standard four-probe method in a temperature range from 77 to 300 K.

3. Results and discussion

In the MOD process, the selection of precursor compounds and solvents is actually important for getting high-quality films, wherein possible chemical interactions in the solution and complicated film growth mechanism during heat treatment process should be considered. In order to determine a reasonable temperature range for the pyrolysis of organic materials in dried films, we performed the thermogravimetric analysis (TGA, 10°C min^{-1} in air) for the lanthanum nitrate $[La(NO_3)_3 \cdot 6H_2O]$, nickel acetate $[Ni(CH_3COO)_3 \cdot 4H_2O]$ and $LaNiO_3$ gel, respectively. Figure 1 illustrates thermogravimetric analysis (TGA) curves for lanthanum nitrate $[La(NO_3)_3 \cdot 6H_2O]$, nickel acetate $[Ni(CH_3COO)_3 \cdot 4H_2O]$ and the gel obtained from the LNO precursor solution after evaporation of acetic acid solvent at 120°C for 8 h. The TG curve of $La(NO_3)_3 \cdot 6H_2O$ indicates a multi-step weight-loss process: below 345°C is the process of stepwise loss of crystallized water to form anhydrous $La(NO_3)_3$ (75·48%, 342°C; calculated: 75·04%), followed by the decomposition of $La(NO_3)_3$ to La_2O_3 (38·01%, 624°C; calculated: 37·62%) in the range of 340–625°C, which is similar basically to the earlier reports (Gao *et al* 1988). For $[Ni(CH_3COO)_3 \cdot 4H_2O]$ a relatively simple TG curve was observed, where the weight loss between 100 and 120°C is generally the release and evaporation of crystallized water (71·23%, 124°C; calculated: 71·04%), and then the evolution and decomposition of acetic acid between 120 and 350°C with the product of NiO and Ni which is finally oxidized to NiO (27·95%, 634°C; calculated: 30·01%) between 350 and 600°C, as observed by Elmasry *et al* (1996). For the $LaNiO_3$ precursor gel, the weight loss below 150°C is due to the loss of residual acetic acid in the precursor gel and the partial loss of crystallized water in the two precursors. The dehydration step of two precursor materials occurs mainly between 150 and 350°C to form individual metal oxides (36·36%, 681°C; calculated: 36·02%). The TGA curve of decomposition of the mixed salts is the overlap of the TG curves for the separate salts, but the decomposition reactions are shifted to lower temperatures,
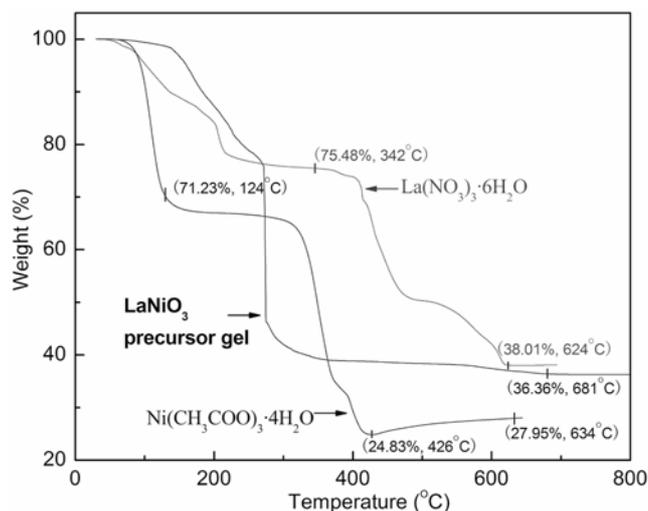

Figure 1. Thermal analysis of $La(NO_3)_3 \cdot 6H_2O$, $Ni(CH_3COO)_2 \cdot 4H_2O$ and $LaNiO_3$ precursor gel.

similar to thermal decomposition behaviors of the mixture of Ni(II) and Fe(III) acetates (Elmasry *et al* 1996). Based on the TGA curves we selected the initial pyrolysis temperature for MOD-LaNiO₃ just above 300°C.

We have chosen two heat treatment temperature points to investigate the decomposition and phase formation in the LaNiO₃ precursor gels. Figure 2 gives XRD patterns of the powders treated at 400 and 700°C for 3 h in air. The sample after firing at 400°C for 3 h displayed several broad diffraction peaks that could be assigned to those of La₂O₃, NiO, Ni₂O₃ or LaNiO₃ phases. It could be said that the precursor gel completely decomposed into the metal oxides together with a little amount of the LaNiO₃ phase at 400°C. Compared to the results of the thermal analysis above, it is found that the decomposition temperature of LaNiO₃ gel is indeed lower than that of each precursor material. With increasing heat treatment temperature up to 700°C, the XRD reflections indexed well according to the LaNiO₃ phase. It means that the LaNiO₃ gel was completely crystallized up to 700°C. The detailed investigation of heat treatments on orientation of MOD-films will be discussed later.

Now we discuss the LaNiO₃ films by MOD with different low-temperature heat treatments between 300 and 450°C, i.e. just higher than the determined initial pyrolysis temperature by TGA technique. The treatment temperature of phase formation is fixed at 700°C. In figure 3 the XRD patterns are plotted for four samples. Only (*h*00)-oriented peaks of the LaNiO₃ phase are observed except for the sample heat-treated at 450°C. The temperature dependence of the (200) peak on the low-temperature heat treatment is shown in the inset of figure 3. The strongest (200) reflection intensity was detected for the sample treated at 350°C. The degree of preferred

orientation *F* (Lotering 1959), first proposed by Lotering, was employed to estimate the film texture here. The *F* value was found to be close to 0·90 for the sample treated at 350°C) (see the inset of figure 3). This indicates that lower or higher heat treatments are destructive for the (*h*00)-oriented films. The heat treatment at lower temperature may result in incomplete decomposition of the LaNiO₃ gels, whereas the heat treatment at higher temperature could lead to non-simultaneous pyrolysis of components in the gels. These two heat treatment profiles are unfavourable for nucleation of oriented LaNiO₃ crystallites.

Figure 4 displays the effect of annealing temperature on the LaNiO₃ film texture prepared by MOD. All samples were heat-treated at 350°C for 2 h in air. The annealing step was carried out at various peak temperatures of *T* = 500–800°C for 3 h in a horizontal furnace. When the annealing temperature is lower than 800°C, the (*h*00) peaks of LaNiO₃ are observed. The strongest (200) reflection occurs for the sample treated at 600°C. At the same time the *F* value reaches a maximum. However, the film annealed at 800°C shows an unknown diffraction peak, which may be due to the decomposition of the LaNiO₃ phase (Cho *et al* 1997).

In order to investigate the effect of film thickness on the film texture, we prepared LaNiO₃ films by multi-coating technique. The precursor film with a single spin coating was first fired at 350°C for 1 h to remove organic components, and then the spin coating was repeated, followed by pyrolysis again at 350°C. This process was repeated several times to achieve desired film thickness from 30 nm to 150 nm. Finally, the fired films were heated at 700°C for 3 h for crystallization. Figure 5 gives XRD patterns of different thick films. It is found that the LNO (*h*00) peaks are dominant in all three different
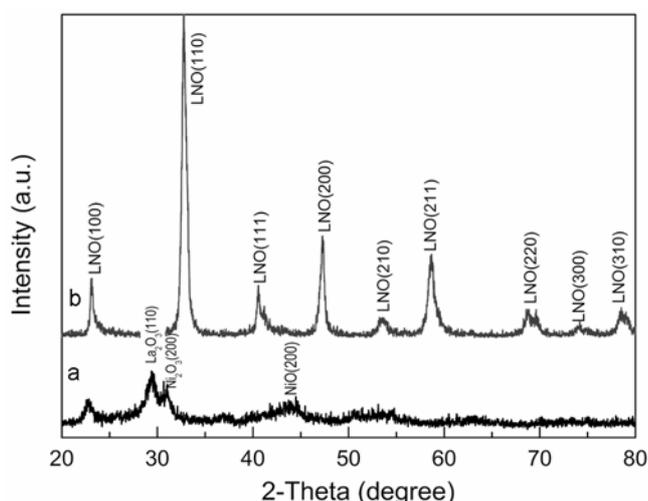

Figure 2. XRD patterns of the powder derived from the LaNiO₃ gel after heat treatments at (a) 400°C and (b) 700°C for 3 h in air.
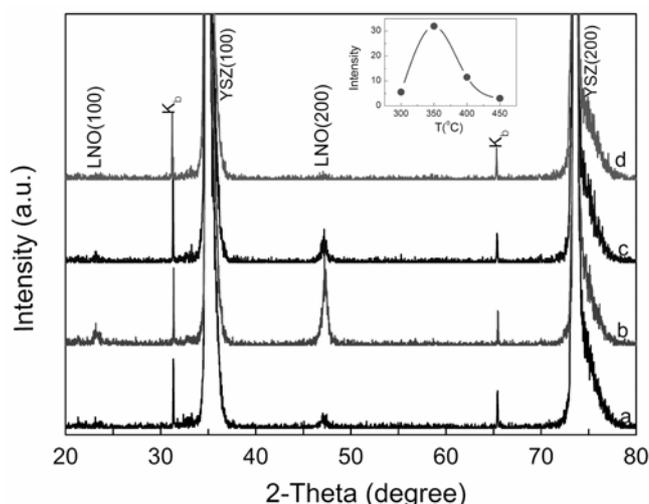

Figure 3. XRD profiles of LaNiO₃ films YSZ (100) heat-treated at (a) 300°C; (b) 350°C; (c) 400°C and (d) 450°C for 3 h, then annealed at 700°C for 1 h in air.

thickness films. However, the thickest film of about 150 nm (five times coating) shows not only the LNO (*h*00) peaks but also the LNO (110) peak. This suggests that the degree of the *c*-axis texture decreases when the thickness of LaNiO$_3$ film is too high. Good (*h*00) orientation of LaNiO$_3$ films can be obtained if the film thickness is not greater than about 100 nm. If we consider a relatively large lattice mismatch of 5.5% between LaNiO$_3$ and YSZ, the (*h*00) orientation of LaNiO$_3$ films might gradually become weak with increasing the film thickness because of possible strain relaxation.

AFM investigations of surface morphology of the LaNiO$_3$ films were carried out and the AFM images are illustrated in figure 6. All images show no cracks and no

pinholes; the LNO surfaces comprise of densely packed round-shaped grains. The surface roughness is about 13 nm for the LNO film heat-treated at 700°C for 3 h
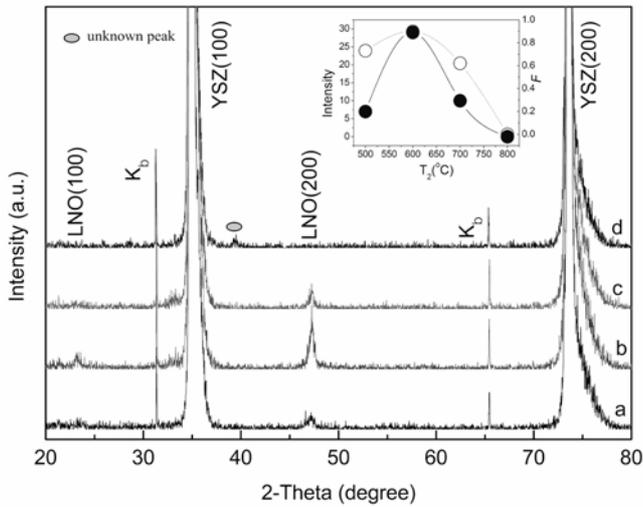

Figure 4. XRD profiles of LaNiO$_3$ films on YSZ (100) substrates initially heat-treated at 350°C for 2 h then annealed at (a) 500°C; (b) 600°C; (c) 700°C and (d) 800°C for 3 h in air.
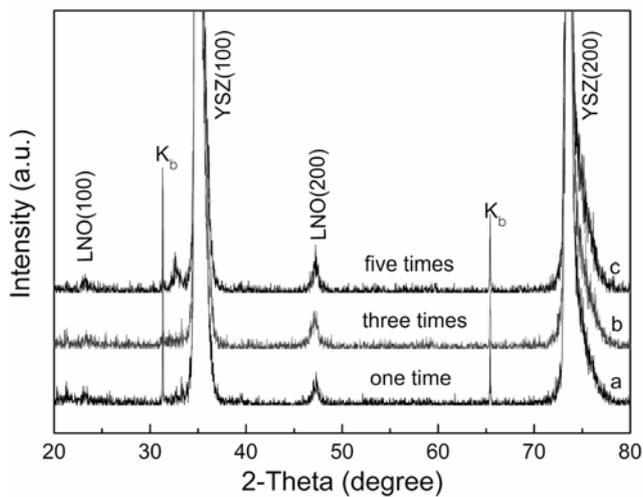

Figure 5. XRD patterns of LaNiO$_3$ films on YSZ (100) with multi-coatings annealed at 700°C after pyrolysis at 350°C.
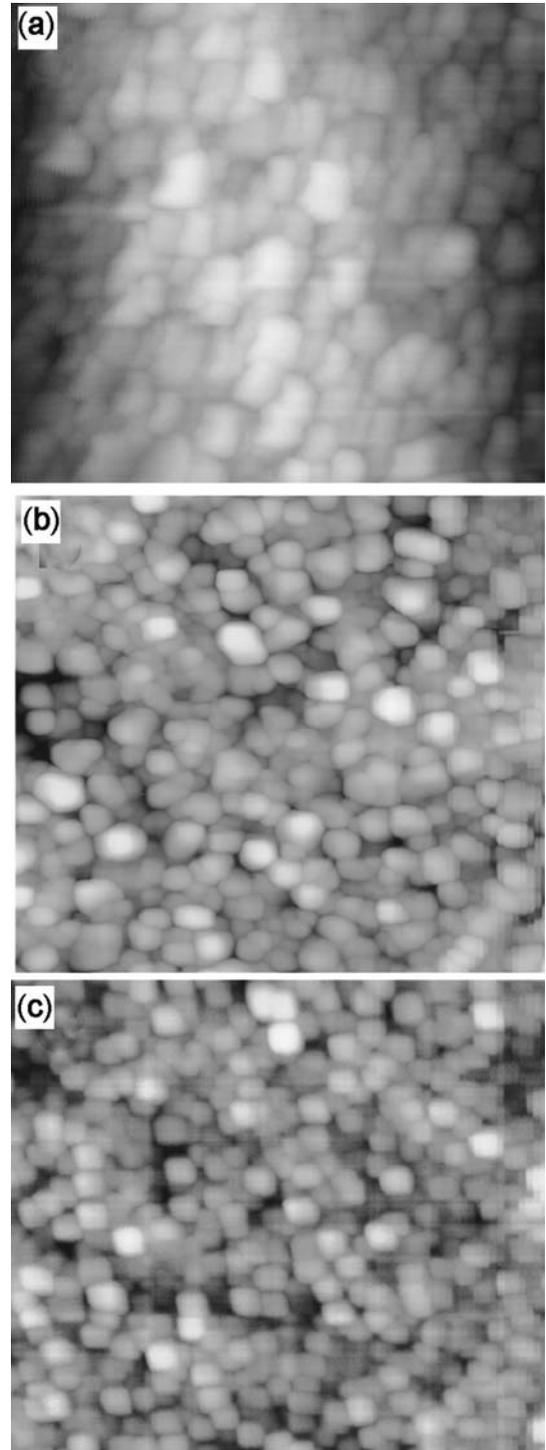

Figure 6. AFM images of LNO films on YSZ (100) substrate with different heat treatments. (**a**) Annealed at 700°C for 3 h without low-temperature heat treatment; (**b**) heat-treated at 350°C for 2 h and then annealed at 700°C for 3 h and (**c**) heat-treated at 350°C for 2 h and then annealed at 600°C for 3 h.
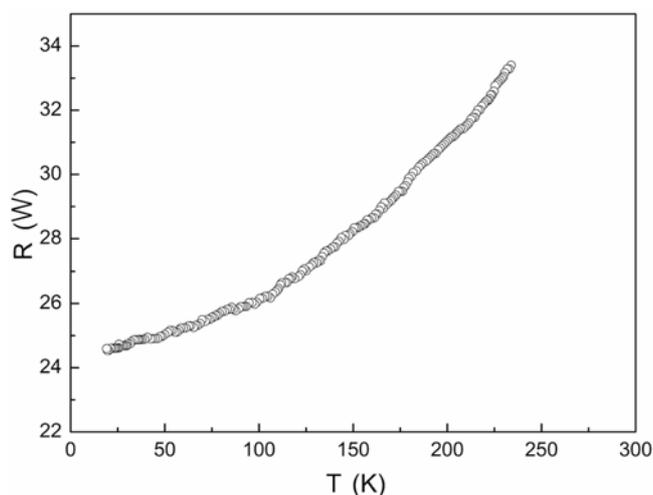
Figure 7. Typical temperature dependence of the electrical resistivity of LaNiO₃ films.

without pyrolysis process (see figure 6a). When the LNO film experienced two-stage heat treatment of pyrolysis at 350°C for 2 h and then of annealing at 700°C for 3 h, the surface roughness of the film decreases down to about 10 nm (see figure 6b). If the annealing temperature of 600°C is used, the surface roughness continues to decrease to 2·5 nm (see figure 6c). Such a low surface roughness of LaNiO₃ films prepared via MOD is comparable with that of films by sputtering technique (Wakiya *et al* 2002).

In order to explore the conductivity of these LaNiO₃ films, we have performed measurements of the electrical resistivity vs temperature as shown in figure 7. The typical $R(T)$ curve displays a monotonic decrease of resistivity with decreasing temperature, which confirms a metallic behaviour like that found in the PVD films (Cho *et al* 1997).

4. Conclusions

In conclusion, the (h00)-orientated LaNiO₃ films on YSZ (100) substrates were successfully fabricated by MOD with high-quality precursor solution. The orientation of LaNiO₃ films is greatly influenced by heat treatment profiles at low and high temperatures, which is related to the processes of decomposition and crystallization. With increasing film thickness, the pure (h00) texture becomes more and more weak. Under optimal conditions, the smooth films of LaNiO₃ with highly (h00) texture

could be obtained. Therefore, the MOD-LaNiO₃ is a potential candidate for buffer layer of YBCO-coated conductors.

References

Bao D, Yao X, Wakiya N, Shinozaki K and Mizutani N 2003 *J. Phys. D. Appl. Phys.* **36** 1217

Berini B, Noun W, Dumont Y, Popova E and Keller N 2007 *J. Appl. Phys.* **101** 023529

Bhuiyan M S, Paranthaman M and Salama K 2006 *Supercond. Sci. Technol.* **19** R1

Cho C R, Payne D A and Cho S L 1997 *Appl. Phys. Lett.* **71** 3013

Elmasry M A A, Gaber A and Khater E M H 1996 *J. Therm. Anal. Calor.* **47** 757

Escote M T, Pontes F M, Leite E R, Varela J A, Jardim R F and Longo E 2003 *Thin Solid Films* **445** 54

Gao S Z and Yang B 1988 *Z. Xibei Jianzhu Gongcheng Xueyuan Yuanbao* **2** 65

Huang H, Yao X, Wang M and Wu X 2004 *J. Cryst. Growth* **263** 406

Knoth K, Hühne R, Oswald S, Schultz L and Holzapfel B 2007 *Acta Mater.* **55** 517

Larbalestier D, Gurevich A, Feldmann D M and Polyanskii A 2001 *Nature* **414** 368

Lee J, Johnson L, Safari A, Ramesh R, Sands T, Gilchrist H and Keramidas V G 1993 *Appl. Phys. Lett.* **63** 27

Li A, Ge C, Lü P and Ming N 1996a *Appl. Phys. Lett.* **68** 1347

Li A, Ge C, Lü P and Ming N 1996b *Appl. Phys. Lett.* **70** 1616

Lotering F K 1959 *J. Inorg. Nucl. Chem.* **9** 113

Meng X J, Cheng J G, Sun J L, Ye H J, Guo S L and Chu J H 2000 *J. Crystal Growth* **220** 100

Miyake S, Yamamoto K, Fujihara S and Kimura T 2002 *J. Am. Ceram. Soc.* **85** 992

Miyazaki H, Goto T, Miwa Y, Ohno T, Suzuki H, Ota T and Takahashi M 2004 *J. Eur. Ceram. Soc.* **24** 1005

Sanchez F, Ferrater C, Guerrero C, Garcia-Cuenca M V and Varela M 2000 *Appl. Phys.* **A71** 59

Wakiya N, Azuma T, Shinozaki K and Mizutani N 2002 *Thin Solid Films* **410** 14

Yu S, Yao K and Tay Eng Hock F 2004 *Ceram. Int.* **30** 1253

Zhang Y, Zhou Q F, Chan H L W and Choy C L 2000 *Thin Solid Films* **375** 87